Redox-Assisted Osmium-Promoted C–C Bond Activation of Alkylnitriles

Juan C. Babón,[†] Miguel A. Esteruelas,*,[†] Israel Fernández,[‡] Ana M. López,[†] and Enrique Oñate[†]

[†]Departamento de Química Inorgánica, Instituto de Síntesis Química y Catálisis Homogénea (ISQCH), Centro de Innovación en Química Avanzada (ORFEO-CINQA), Universidad de Zaragoza-CSIC, 50009 Zaragoza, Spain

[‡]Departamento de Química Orgánica I, Facultad de Ciencias Químicas, Centro de Innovación en Química Avanzada (ORFEO-CINQA), Universidad Complutense de Madrid, 28040 Madrid, Spain

Supporting Information Placeholder

ABSTRACT: The redox-assisted $C(sp)$–$C(sp^3)$ bond activation of alkylnitriles coordinated to osmium(II)-dihydride fragments has been performed with an osmium(VI)-polyhydride to liberate alkanes and generate dinuclear complexes formed by two osmium(IV)-polyhydride moieties linked by only one CN-bridge. In addition, the bonding situation in these novel dinuclear species has been computationally studied.

The high directionality of the σ-orbital of the C–C single bond, constrained straightway along the axis, prevents its interaction with transition metals.[1] As a consequence, although a variety of approaches have been used in order to solve the issue,[2] the C–C cleavage is the least frequent among the transition metal mediated σ-bond activation processes.[3] In this context, the development of procedures and complexes for promoting the C–CN bond rupture is of particular interest since this bond is present in many organic molecules and their decyanation is crucial in organic synthesis.[4] Thus, a number of complexes,[5] mainly of groups 9 and 10, have been employed to activate C–CN bonds. Two strategies have been vastly followed (Scheme 1): i) oxidative addition of the C–CN bond[6] to Rh(-I),[7] Co(I),[8] Rh(I),[9] Ni(0),[10] Pd(0),[11] Pt(0)[12] and ii) insertion of the C–N triple bond into M–SiR$_3$ (Fe,[13] Rh[14]) or Rh–BR$_2$[15] bonds followed by α-carbon elimination. In this communication, we wish to report on a different procedure which applies to osmium (iii in Scheme 1).

Addition reactions are visualized as processes where double or triple bonds are fully or partially broken in order to accommodate additional atoms or group of atoms thus forming a larger molecule. Sometimes the addition is accompanied by the loss of a small fragment. Then, the process is known as an addition-elimination reaction. The coordination of an organic molecule to a transition metal changes the chemical behavior of both the organic molecule and the metal center. In agreement with this, we have observed an unusual 1,3-addition-4-elimination reaction, which takes places between alkylnitriles coordinated to an osmium(II) center and a osmium(VI) polyhydride. The reaction produces the elimination of alkane as a result of the $C(sp^3)$–$C(sp)$ bond activation of the nitrile and the comproportionation of the metal centers to osmium(IV). To-
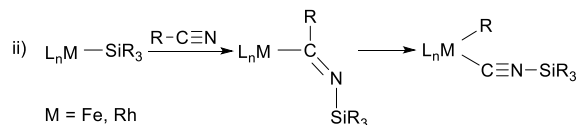
gether, both processes yield dinuclear polyhydrides with a CN-bridge, in addition to the saturated hydrocarbon.

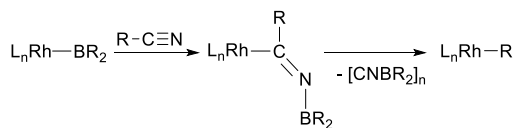**Scheme 1. $C(sp)$–$C(sp^3)$ Bond Activation of Alkylnitriles**
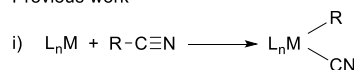
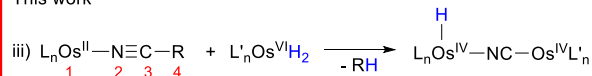Hexahydride complex $OsH_6(P^iPr_3)_2$ (**1**)[16] loses two hydrogen molecules in acetonitrile:toluene (1:1) at 130 °C. The resulting 14e metal fragment $OsH_2(P^iPr_3)_2$ is trapped by the nitrile to form the *cis*-dihydride-bis(acetonitrile) derivative $OsH_2(MeCN)_2(P^iPr_3)_2$ (**2**). The coordination of the nitrogen atom of the nitrile to the osmium atom enhances the electrophilicity of the $C(sp)$-atom, which increases its susceptibility towards the nucleophilic attack of a new hexahydride molecule. The addition facilitates a double hydrogen transfer from

the osmium(VI) center, which undergoes reduction to osmium(IV). One of the hydrogen transfers takes place to the osmium(II) center of the dihydride, which is oxidized to osmium(IV), whereas the other one has the methyl substituent of the nitrile as a hydrogen acceptor, which is liberated as methane. Thus, the treatment of toluene solutions of **1** with 1.0 equiv. of **2**, at 60 °C, for 24h leads to the dinuclear polyhydride (P^{i}Pr$_3$)$_2$H$_4$Os(μ-CN)OsH$_3$(MeCN)(P^{i}Pr$_3$)$_2$ (**3**) and methane, in almost quantitative yield according to the ^{31}P{^{1}H} NMR spectrum of the reaction crude. Its formation is the result of the comproportionation of the metal centers and the C–C bond activation of one of the coordinated nitriles (Scheme 2).

Scheme 2. C(sp)–C(sp^3) Bond Activation of Coordinated Acetonitrile Promoted by 1
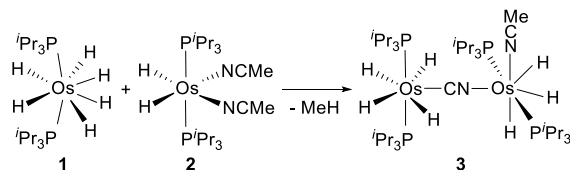
Complex **3** was characterized by X-ray diffraction analysis. Figure 1 gives a view of the molecule. The structure proves the formation of the cyano ligand, which affords a linear Os(1)–N(1)–C(1)–Os(2) bridge with Os(1)–N(1)–C(1) and N(1)–C(1)–Os(2) angles of 176.9(4)° and 178.1(4)°, respectively, and a N(1)–C(1) distance of 1.152(6) Å. In agreement with the +4 oxidation state of both metal centers, the coordination polyhedra around the osmium atoms can be rationalized as distorted pentagonal bipyramids with axial phosphines (P(1)–Os–P(2) = 167.99(5)° and P(3)–Os–P(4) = 167.68(5)°). The metal coordination sphere around Os(1) is completed by three hydride ligands, an acetonitrile molecule, and the nitrogen atom of the cyano group, whereas the metal coordination sphere around Os(2) is completed by four hydride ligands and the carbon atom of the cyano group. The equatorial planes form an angle of 53.12°. In the ^{13}C{^{1}H} NMR spectrum, the C(1) atom gives rise to a triplet ($^2J_{C-P}$ = 7.7 Hz) at 141.2 ppm. According to the presence of the OsH$_4$P$_2$ and OsH$_3$P$_2$ moieties, the ^{1}H NMR spectrum contains two hydride resonances at -11.03 (t, $^3J_{H-P}$ = 14.5 Hz) and -12.41 (t, $^3J_{H-P}$ = 12.4 Hz) ppm in a 4:3 intensity ratio and the ^{31}P{^{1}H} NMR spectrum shows two signals at 42.4 and 26.0 ppm.
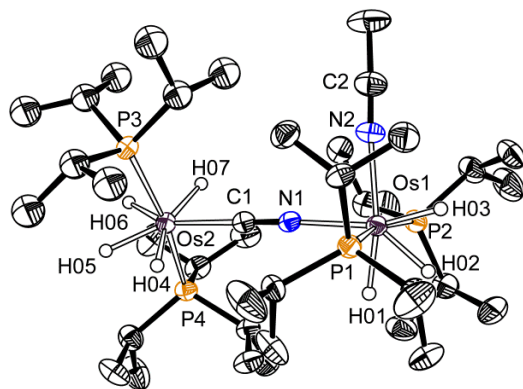

Figure 1. Molecular diagram of complex **3** with 50% probability ellipsoids. Hydrogen atoms (except hydrides) are omitted for clarity. Selected bond lengths (Å) and angles (deg): Os(1)–N(1) =

2.134(4), Os(1)–N(2) = 2.138(4), Os(2)–C(1) = 2.074(5), N(1)–C(1) = 1.152(6), N(2)–C(2) = 1.122(7); Os(1)–N(1)–C(1) = 176.9(4), N(1)–C(1)–Os(2) = 178.1(4), P(1)–Os(1)–P(2) = 167.99(5), P(3)–Os(2)–P(4) = 167.68(5).

The bonding situation in complex **3** was analyzed by DFT calculations using the Atoms in Molecules (AIM), Natural Bond Orbital (NBO), and Energy Decomposition Analysis-Natural Orbital for Chemical Valence (EDA-NOCV) methods.[17]

Figure 2 shows the Laplacian distribution in the Os–C–N–OsH$_3$ plane. As expected, the AIM method locates bond critical points (BCPs) together with the associated bond paths (BPs) between the transition metals and the carbon and nitrogen atoms. Both Os–N and Os–C bonds show areas of charge concentration ($\nabla^2\rho(r) < 0$, dashed lines) at the nitrogen and carbon ends, which have the shape of a droplet-like appendix directed toward the osmium atom, a topology which is typical for a closed-shell donor acceptor interaction.[18] The C–N bond of the cyano group is weaker than that of the acetonitrile ligand, as revealed by the computed respective NBO-Wiberg Bond Indexes (WBI) of 2.49 and 2.63. Not surprisingly, both C–N bonds are weaker than that computed for free MeCN (WBI = 2.88), which nicely reflects the effect of the coordination into the C–N bond strength. Bond critical points and bond paths were not located between the hydride ligands, in agreement with their classical nature.
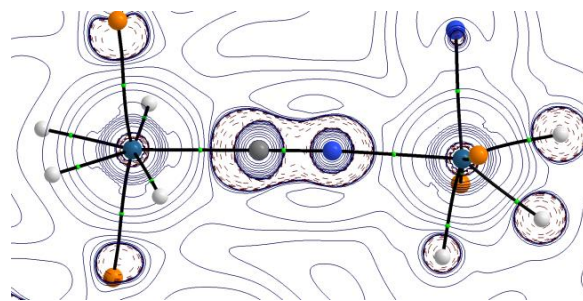

Figure 2. Contour line diagrams $\nabla^2\rho(r)$ for complex **3** in the Os−C–N–OsH$_3$ plane computed at the BP86-D3/def2-SVP level. Solid lines indicate areas of charge depletion ($\nabla^2\rho(r) > 0$) while dashed lines show areas of charge concentration ($\nabla^2\rho(r) < 0$). The solid lines connecting the atomic nuclei are the bond paths while the small green spheres indicate the corresponding bond critical points.

The EDA-NOCV method was applied next in order to confirm the donor-acceptor nature of the Os–N and Os–C bonds and to gain more quantitative insight into the bonding situation of the novel dinuclear species. The bonds were analyzed in two different partitioning schemes using either neutral or charged fragments. The calculation that gives the smallest orbital form ΔE_{orb} (i.e. involving the smallest change in the electronic structure of the fragments by the bond formation) indicates the most reasonable description of the bond. According to the results collected in Table 1, both Os–N and Os–C bonds are best described using closed-shell fragments, charged fragments for the Os–N bond ([(P^{i}Pr$_3$)$_2$H$_4$Os]CN$^-$ and [OsH$_3$(MeCN)(P^{i}Pr$_3$)$_2$]$^+$) and neutral fragments for the Os–C bond ([(P^{i}Pr$_3$)$_2$H$_4$Os] and CN[OsH$_3$(MeCN)(P^{i}Pr$_3$)$_2$]), which confirms their dative nature. Interestingly, for both bonds, the electrostatic form ΔE_{elstat} becomes the major contributor to the total interaction, indicating the highly polar nature of the Os–C

Table 1. EDA-NOCV Results (in kcal/mol) Computed at the ZORA-BP86-D3/TZ2P+//BP86-D3/def2-SVP Level

	Os–N bond		Os–C bond	
	Electron-sharing	Dative bond	Electron-sharing	Dative bond
Fragments	$[(P^iPr_3)_2H_4Os]CN^{\bullet}$ $[OsH_3(MeCN)(P^iPr_3)_2]^{\bullet}$	$[(P^iPr_3)_2H_4Os]CN^-$ $[OsH_3(MeCN)(P^iPr_3)_2]^+$	$[(P^iPr_3)_2H_4Os]^{\bullet+}$ $CN[OsH_3(MeCN)(P^iPr_3)_2]^{\bullet-}$	$[(P^iPr_3)_2H_4Os]$ $CN[OsH_3(MeCN)(P^iPr_3)_2]$
ΔE_{int}	-104.4	-136.1	-233.4	-83.7
ΔE_{Pauli}	238.8	140.9	213.7	200.0
$\Delta E_{elstat}{}^a$	-129.1 (37.6%)	-163.0 (58.9%)	-223.7 (49.9%)	-159.2 (56.1%)
$\Delta E_{orb}{}^a$	-176.3 (51.4%)	-76.1 (27.5%)	-188.6 (42.1%)	-88.7 (31.3%)
$\Delta E_{disp}{}^a$	-37.8 (11.0%)	-37.8 (13.6%)	-35.8 (8.0%)	-35.8 (12.6%)
$\Delta E_{orb}(\rho_1)^b$		–37.5 (49.3%)		-47.9 (54.0%)
$\Delta E_{orb}(\rho_2)^b$		–6.1 (8.0%)		-12.6 (14.3%)

^{a}The values within parentheses indicate the percentage to the total attractive interaction energy, $\Delta E_{int} = \Delta E_{Pauli} + \Delta E_{elstat} + \Delta E_{orb} + \Delta E_{disp}$.
^{b}The values in parentheses give the percentage contribution to the total orbital interactions ΔE_{orb}.

and Os–N interactions. Moreover, the orbital interactions can be visualized and quantified by means of the NOCV method.

Figure 3 shows the main computed deformation densities $\Delta\rho$ (the charge flow takes place in the direction red → blue) for both bonds. The Os–C bond (Fig. 3a) can be viewed as a σ-bond, which involves the donation of electron density from the LP(C) to a vacant σ* molecular orbital of the transition metal fragment $[(P^iPr_3)_2H_4Os]$, having a small π-backbonding to the vacant p_z(C) atomic orbital. A similar bonding description is found for the Os–N bond (Fig. 3b).
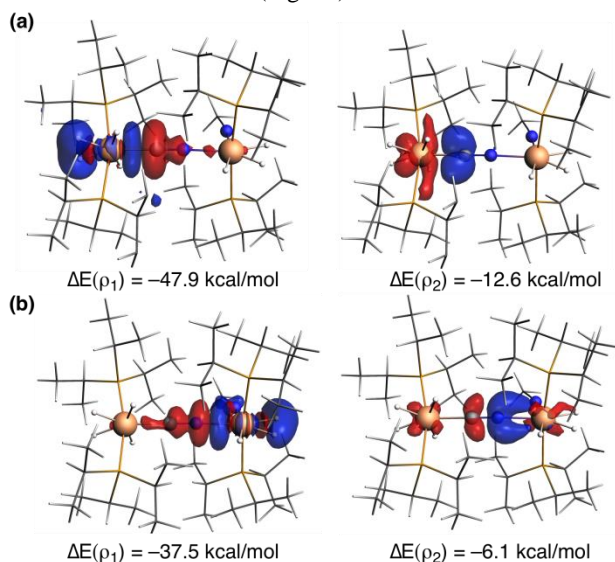

Figure 3. NOCV-deformation densities for bond Os–C (a) and Os–N (b) in complex **3**. The charge flow takes place in the direction red → blue.

Complex **3** can be also obtained in a one-pot synthesis procedure at 60 °C, starting from **1** and acetonitrile. Thus, treatment of the hexahydride with 2.0 equiv. of the nitrile at this temperature affords the dinuclear species in about 50% yield, after 48h, according to the $^{31}P\{^1H\}$ NMR spectrum of the reaction mixture. Under similar reaction conditions, complex **1** also activates the C(sp)–C(sp^3) bond of propionitrile to release ethane and yield the dinuclear compound $(P^iPr_3)_2H_4Os(\mu$-CN)OsH_3(EtCN)(P^iPr_3)_2$ (**4**), containing a propionitrile mole-

cule in the analogous position to the acetonitrile ligand in complex **3** (Scheme 3).

Scheme 3. One-Pot Synthesis of the Dinuclear Complexes 3 and 4 Starting from 1 and Nitriles
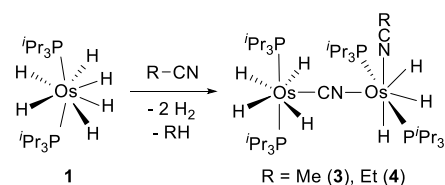
In conclusion, a novel procedure to perform the C(sp)–C(sp^3) bond activation of alkylnitriles has been discovered. It applies to the d^2-hexahydride OsH_6(P^iPr_3)_2 complex and has afforded the first transition metal dinuclear complexes formed by two polyhydride moieties linked by a CN-bridge.

ASSOCIATED CONTENT

Supporting Information

The Supporting Information is available free of charge on the ACS Publications website.

Experimental details, NMR data of complexes **2-4**, crystal data for **3** and computational details (PDF)
Cartesian coordinates of 3 (XYZ)

Accesion codes

CCDC 1838027 contains the supplementary crystallographic data for this paper. These data can be obtained free of charge via www.ccdc.cam.ac.uk/data_request/cif, or by emailing data_request@ccdc.cam.ac.uk, or by contacting The Cambridge Crystallographic Data Centre, 12 Union Road, Cambridge CB2 1EZ, UK; fax: +44 1223 336033.

AUTHOR INFORMATION

Corresponding Author

*E-mail for M.A.E.: maester@unizar.es
Notes
The authors declare no competing financial interest.

REFERENCES

(1) Harvey, B. G.; Ernst, R. D. Transition-Metal Complexes with (C–C)→M Agostic Interactions. *Eur. J. Inorg. Chem.* **2017**, 1205-1226.

(2) (a) Crabtree, R. H. The Organometallic Chemistry of Alkanes. *Chem. Rev.* **1985**, *85*, 245-269. (b) Murakami, M. Ito, Y. Cleavage of Carbon–Carbon Single Bonds by Transition Metals. *Top. Organomet. Chem.* **1999**, *3*, 97-129. (c) Rybtchinski, B.; Milstein, D. Metal Insertions into C–C Bonds in Solution. *Angew. Chem., Int. Ed.* **1999**, *38*, 870-883. (d) Ruhland, K. Transition-Metal-Mediated Cleavage and Activation of C–C Single Bonds. *Eur. J. Org. Chem.* **2012**, 2683-2706. (e) Esteruelas, M. A.; Oñate, E.; Palacios, A. U. Alkenyl-Assisted C^3–C Bond Activation of Acetylacetonate Coordinated to Iridium. *Organometallics* **2017**, *36*, 4344-4347.

(3) Esteruelas, M. A.; López, A. M.; Oliván, M. Polyhydrides of Platinum Group Metals: Nonclassical Interactions and σ-Bond Activation Reactions. *Chem. Rev.* **2016**, *116*, 8770-8847.

(4) (a) Chen, F.; Wang, T.; Jiao, N. Recent Advances in Transition-Metal-Catalyzed Functionalization of Unstrained Carbon–Carbon Bonds. *Chem. Rev.* **2014**, *114*, 8613-8661. (b) Wen, Q.; Lu, P.; Wang, Y. Recent advances in transition-metal-catalyzed C–CN bond activations. *RSC Adv.* **2014**, *4*, 47806-47826.

(5) (a) Churchill, D.; Shin, J. H.; Hascall, T.; Hahn, J. M.; Bridgewater, B. M.; Parkin, G. The *Ansa* Effect in Permethylmolybdenocene Chemistry: A [Me$_2$Si] *Ansa* Bridge Promotes Intermolecular C–H and C–C Bond Activation. *Organometallics* **1999**, *18*, 2403-2406. (b) Yang, L.-Z.; Li, Y.; Zhuang, X.-M.; Jiang, L.; Chen, J. M.; Luck, R. L.; Lu, T. B. Mechanistic Studies of C–C Bond Cleavage of Nitriles by Dinuclear Metal Cryptates. *Chem. - Eur. J.* **2009**, *15*, 12399-12407. (c) Guo, L. R.; Bao, S.-S.; Li, Y.-Z.; Zheng, L.-M. Ag(I)-mediated formation of pyrophosphonate coupled with C–C bond cleavage of acetonitrile. *Chem. Commun.* **2009**, 2893-2895. (d) Xu, F.; Tao, T.; Zhang, K.; Wang, X.-X.; Huang, W.; You, X.-Z. C–C bond cleavage in acetonitrile by copper(II)–bipyridine complexes and *in situ* formation of cyano-bridged mixed-valent copper complexes. *Dalton Trans.* **2013**, *42*, 3631-3645. (e) Heath, R.; Müller-Bunz, H.; Albrecht, M. Silver(I) NHC mediated C–C bond activation of alkyl nitriles and catalytic efficiency in oxazoline synthesis. *Chem. Commun.* **2015**, *51*, 8699-8701.

(6) Souillart, L.; Cramer, N. Catalytic C–C Bond Activations via Oxidative Addition to Transition Metals. *Chem. Rev.* **2015**, *115*, 9410-9464.

(7) Grochowski, M. R.; Morris, J.; Brennessel, W. W.; Jones, W. D. C–CN Bond Activation of Benzonitrile with [Rh$^{–1}$(dippe)]$^–$. *Organometallics* **2011**, *30*, 5604-5610.

(8) Xu, H. W.; Williard, P. G.; Bernskoetter, W. H. C–CN Bond Activation of Acetonitrile using Cobalt(I). *Organometallics* **2012**, *31*, 1588-1590.

(9) (a) Evans, M. E.; Li, T.; Jones, W. D. C–H vs C–C Bond Activation of Acetonitrile and Benzonitrile via Oxidative Addition: Rhodium vs Nickel and Cp* vs Tp′ (Tp′ = Hydrotris(3,5-dimethylpyrazol-1-yl)borate, Cp* = η^5-Pentamethylcyclopentadienyl). *J. Am. Chem. Soc.* **2010**, *132*, 16278-16284. (b) Evans, M. E.; Jones, W. D. Controlling the Selectivity for C–H and C–CN Bond Activation at Rhodium: A DFT Examination of Ligand Effects. *Organometallics* **2011**, *30*, 3371-3377.

(10) (a) Garcia, J. J.; Brunkan, N. M.; Jones, W. D. Cleavage of Carbon−Carbon Bonds in Aromatic Nitriles Using Nickel(0). *J. Am. Chem. Soc.* **2002**, *124*, 9547-9555. (b) Brunkan, N. M.; Brestensky, D. M.; Jones, W. D. Kinetics, Thermodynamics, and Effect of BPh$_3$ on Competitive C−C and C−H Bond Activation Reactions in the Interconversion of Allyl Cyanide by [Ni(dippe)]. *J. Am. Chem. Soc.*

2004, *126*, 3627-3641. (c) Atesin, T. A.; Li, T.; Lachaize, S.; Brennessel, W. W.; García, J. J.; Jones, W. D. Experimental and Theoretical Examination of C−CN and C−H Bond Activations of Acetonitrile Using Zerovalent Nickel. *J. Am. Chem. Soc.* **2007**, *129*, 7562-7569. (d) Schaub, T.; Döring, C.; Radius, U. Efficient nickel mediated carbon–carbon bond cleavage of organonitriles. *Dalton Trans.* **2007**, 1993-2002. (e) Swartz, B. D.; Reinartz, N. M.; Brennessel, W. W.; García, J. J.; Jones, W. D. Solvent Effects and Activation Parameters in the Competitive Cleavage of C-CN and C-H Bonds in 2-Methyl-3-Butenenitrile Using [(dippe)NiH]$_2$. *J. Am. Chem. Soc.* **2008**, *130*, 8548-8554. (f) Li, T.; García, J. J.; Brennessel, W. W.; Jones, W. D. C−CN Bond Activation of Aromatic Nitriles and Fluxionality of the η^2-Arene Intermediates: Experimental and Theoretical Investigations. *Organometallics* **2010**, *29*, 2430-2445. (g) Fang, X. J.; Yu, P.; Morandi, B. Catalytic reversible alkene-nitrile interconversion through controllable transfer hydrocyanation. *Science* **2016**, *351*, 832-836. (h) Ni, S.-F.; Yang, T.-L.; Dang, L. Transfer Hydrocyanation by Nickel(0)/Lewis Acid Cooperative Catalysis, Mechanism Investigation, and Computational Prediction of Shuttle Catalysts. *Organometallics* **2017**, *36*, 2746-2754.

(11) Munjanja, L.; Torres-López, C.; Brennessel, W. W.; Jones, W. D. C–CN Bond Cleavage Using Palladium Supported by a Dippe Ligand. *Organometallics* **2016**, *35*, 2010-2013.

(12) Swartz, B. D.; Brennessel, W. W.; Jones, W. D. C−CN vs C−H Cleavage of Benzonitrile Using [(dippe)PtH]$_2$. *Organometallics* **2011**, *30*, 1523-1529.

(13) Nakazawa, H.; Itazaki, M.; Kamata, K.; Ueda, K. Iron-Complex-Catalyzed C–C Bond Cleavage of Organonitriles: Catalytic Metathesis Reaction between H–Si and R–CN Bonds to Afford R–H and Si–CN Bonds. *Chem.- Asian J.* **2007**, *2*, 882-888.

(14) Taw, F. L.; Mueller, A. H.; Bergman, R. G.; Brookhart, M. A Mechanistic Investigation of the Carbon−Carbon Bond Cleavage of Aryl and Alkyl Cyanides Using a Cationic Rh(III) Silyl Complex. *J. Am. Chem. Soc.* **2003**, *125*, 9808-9813.

(15) Esteruelas, M. A.; Oliván, M.; Vélez, A. Conclusive Evidence on the Mechanism of the Rhodium-Mediated Decyanative Borylation. *J. Am. Chem. Soc.* **2015**, *137*, 12321-12329.

(16) Aracama, M.; Esteruelas, M. A.; Lahoz, F. J.; López, J. A.; Meyer, U.; Oro, L. A.; Werner, H. Synthesis, Reactivity, Molecular Structure, and Catalytic Activity of the Novel Dichlorodihydridoosmium(IV) Complexes OsH$_2$Cl$_2$(PR$_3$)$_2$ (PR$_3$ = P-*i*-Pr$_3$, PMe-*t*-Bu$_2$). *Inorg. Chem.*, **1991**, *30*, 288−293.

(17) See Computacional Details.

(18) (a) Braunschweig, H.; Fernández, I.; Frenking, G.; Radacki, K.; Seeler, F. Synthesis and Electronic Structure of a Ferroborirene. *Angew. Chem., Int. Ed.* **2007**, *46*, 5215-5218. (b) Esteruelas, M. A.; Fernández, I.; Herrera, A.; Martín-Ortiz, M.; Martínez-Álvarez, R.; Oliván, M.; Oñate, E.; Sierra, M. A.; Valencia, M. Multiple C−H Bond Activation of Phenyl-Substituted Pyrimidines and Triazines Promoted by an Osmium Polyhydride: Formation of Osmapolycycles with Three, Five, and Eight Fused Rings. *Organometallics* **2010**, *29*, 976-986.

Table of Contents artwork